Highly Phase Stable Mode-Locked Lasers

Tara M. Fortier, David J. Jones, Jun Ye, and S. T. Cundiff

***Abstract*—The authors report on stabilizing the carrier-envelope phase of mode-locked Ti:sapphire lasers. Optimization of the construction of the lasers for ease of phase stabilization is discussed. Results demonstrating long-term phase coherence of the generated pulse train are presented, yielding a phase coherence time of at least 326 s, measurement time limited. The conversion of amplitude noise to phase noise in the microstructured fiber, which is used to obtain an octave spanning spectrum, is measured. The resulting phase noise is found to be sufficiently small so as to not corrupt the phase stabilization. Shift of carrier-envelope phase external to the laser cavity due to propagation through a dispersive material is measured.**

***Index Terms*—Carrier-envelope phase stabilization, mode-locked lasers, phase noise.**

I. Introduction

THERE HAS been significant progress over the last few years in stabilizing the carrier-envelope phase of mode-locked lasers [1]–[5]. This has led to remarkable advances in optical frequency metrology [3], [6]–[12] and optical atomic clocks [13]–[15]. At first, this may seem surprising as mode-locked lasers produce ultrashort optical pulses, with very large bandwidth, whereas the latter topics require extremely well-defined frequencies. This discrepancy is resolved by considering the fact that mode-locked lasers produce a train of pulses, not a single pulse. As a consequence, the resulting frequency spectrum does not have a continuous distribution, but rather consists of a "comb" of well-defined frequency components. The pulse-to-pulse evolution of the carrier-envelope phase is manifest in the frequency spectrum as a rigid shift of the comb [2], [16]. In addition to these successes, this technology still has significant promise to impact ultrafast science by allowing the exploration of processes that are sensitive to the carrier-envelope phase. These include extreme nonlinear optics, where the electric field of the pulse is relevant [17], and coherent control. However, these applications require a high degree of carrier-envelope phase coherence, which, in contrast, is less of an issue for frequency domain applications.

A. Background

The concept of the carrier-envelope phase, $\phi_{\rm CE}$, relies on the decomposition of the optical pulse into an envelope and carrier. For a sufficiently short optical pulse, the envelope provides a suitably well-defined phase reference. Due to dispersion in the laser cavity, $\phi_{\rm CE}$ undergoes pulses-to-pulse evolution by an amount $\Delta\phi_{\rm CE}$, as shown in Fig. 1(a). Although $\Delta\phi_{\rm CE}$ is typically much larger than 2π, it only matters modulo 2π. Stabilization of $\phi_{\rm CE}$ corresponds to locking $\Delta\phi_{\rm CE}$, which is done in the frequency domain.

To understand how $\Delta\phi_{\rm CE}$ is manifested in the frequency spectrum, we must look at the frequency spectrum of the entire pulse train emitted by the laser, not just a single pulse. Of course, a single short pulse, with duration T, has a broad spectrum with width proportional to $1/T$. However, the repetitive pulse train results in a "comb" of equally spaced lines in the spectrum [see Fig. 1(b)]. The relative amplitudes of these comb lines are determined by the spectrum of a single pulse and their spacing is just the repetition rate, $f_{\rm rep}$. The pulse-to-pulse evolution of the $\phi_{\rm CE}$ results in a rigid shift of the comb spectrum by an amount $f_0 = f_{\rm rep}\Delta\phi_{\rm CE}/2\pi$ from being integer multiples of the repetition rate. For a detailed derivation, see [16]. This means that the optical frequency of a given comb line is given by

$$\nu_n = n \cdot f_{\rm rep} + f_0 \tag{1}$$

where n is a large integer of order 10^6 that indexes the comb lines. The connection between time and frequency is summarized in Fig. 1. Carrier-envelope phase stabilization of a laser consists of detecting f_0 and then implementing a feedback loop to lock it to a desired value.

B. Detection of f_o

The simplest scheme for detecting f_0 is known as self-referencing [2], [3] and the easiest implementation of self-referencing requires an optical spectrum that spans an octave. Techniques for generating an octave are discussed below. Given an octave spanning spectrum, the low frequency end of spectrum is frequency doubled in an external second harmonic crystal and then heterodyned with the high frequency end of the spectrum. If the index of the low-frequency comb line is n, the comb line closest to its second harmonic has an index $2n$, thus the frequency of the beat is $2\nu_n - \nu_{2n} = 2(n \cdot f_{\rm rep} + f_0) - (2n \cdot f_{\rm rep} + f_0) = f_0$. Since this compares frequencies ν and 2ν, we designate the interferometer that implements it as a ν-to- 2ν interferometer. Higher order implementations of this are possible, for example comparing 2ν to 3ν[18], [19], requiring less bandwidth but more nonlinear steps, which can be a significant disadvantage.

II. Stabilized Laser

Traditionally, the design of a mode-locked laser has not striven for interferometric stability, which is in contrast to the typical case for single frequency continuous-wave (CW) lasers. However, $\phi_{\rm CE}$ is sensitive to phase perturbations, thus it is greatly advantageous to start with a laser that is as passively stable as possible. This is the well-known principle in the

Manuscript received January 10, 2003; revised June 16, 2003. This work was supported in part by the National Institute of Standards and Technology, by ONR, by the National Science Foundation, and by the Defense Advanced Research Project Agency.

The authors are with JILA, the National Institute of Standards and Technology and the University of Colorado, Boulder, CO 80309-0440 USA.

Digital Object Identifier 10.1109/JSTQE.2003.819110

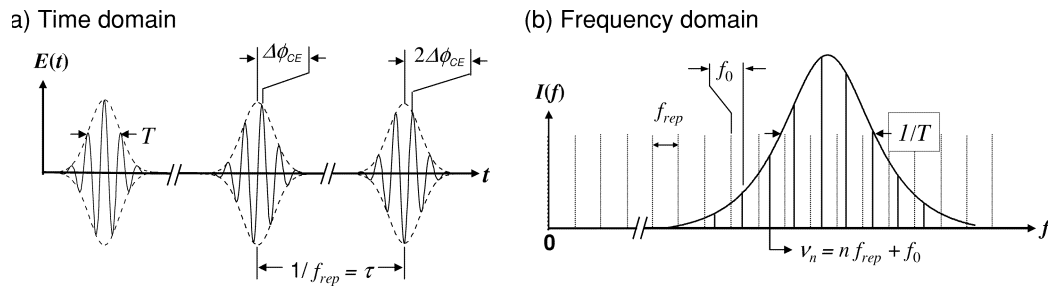

Fig. 1. Time–frequency correspondence between the pulse train and frequency comb and the relationship between $\Delta\phi_{\rm CE}$ and f_0. (a) In the time domain, the relative phase between the carrier and the envelope evolves from pulse to pulse by the amount $\Delta\phi_{\rm CE}$ due to an inequality of intracavity group and phase velocities. (b) In the frequency domain, the elements of the frequency comb of a mode-locked pulse train are spaced by $f_{\rm rep}$. Entire comb is offset from integer multiples of $f_{\rm rep}$ by an offset frequency, f_0. Analysis shows $f_0 = f_{\rm rep}\Delta\phi_{\rm CE}/2\pi$. Without active stabilization, f_0 is a dynamic quantity, which is sensitive to perturbations of the laser. Hence, $\Delta\phi_{\rm CE}$ changes in a nondeterministic manner from pulse to pulse in an unstabilized laser.

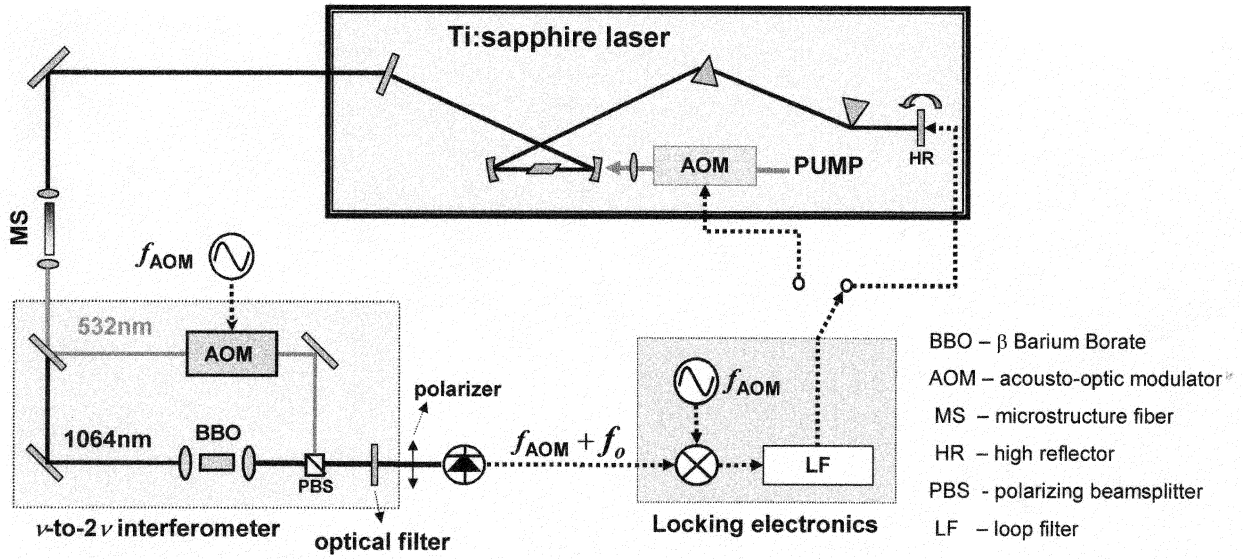

Fig. 2. Experimental apparatus of a carrier-envelope phase-stabilized fs Ti:sapphire laser. Box in the lower left shows the ν-to- 2ν interferometer used to measure f_0. An octave-spanning comb, generated by microstructure fiber, is spectrally separated using a dichroic mirror. Authors used wavelengths centered at 1064 nm for ν and 532 nm for 2ν. S/N of f_0 is optimized by slightly changing these wavelengths. Infrared portion is frequency doubled with a β-barium borate (BBO) crystal and then polarization multiplexed with the existing 2ν signal. Combined beam passes through an interference filter (centered at 2ν) to reject any nonspectrally overlapped comb components. Acousto-optic modulator (AOM) is placed in the visible arm to enable the heterodyne beat to be measured unambiguously.

control community that the best control is achieved for plants that do not need feedback control in the first place.

Kerr-lens mode-locked (KLM) Ti:sapphire lasers [20], [21], the work horse of the ultrafast community, are typically the basis for phase stabilization. Laser designs that incorporate a prism sequence for dispersion compensation [22], [23] and those that employ dispersion compensating mirrors [24]–[27] are used. For optical frequency metrology, high-repetition rate ring cavity designs [28] present advantages, mainly because of the fact that there is more power per comb element. For the work presented here, prism-based lasers are used exclusively. The layout of a typical laser is shown in Fig. 2 together with the stabilization apparatus described below. The exact value of $f_{\rm rep}$ is not important for the measurements but was between 88 and 100 MHz for all of the results presented here.

A. Design Considerations for Phase Stability

The three primary factors affecting phase stability are mechanical vibrations, air pressure changes, and temperature changes. The vibration is addressed by using low profile and solid mirror mounts throughout the laser cavity, which is not typical practice for ultrafast lasers. Of course, high-quality optical tables with vibration isolation legs are required. Enclosing the laser in a rigid box helps to reduce acoustic noise and also addresses the problem of air pressure changes. Air pressure change is detrimental because it alters the density of the air in the cavity, which, in turn, changes the effective path length due to the index of refraction of air. Although this is a small effect, it can easily change the cavity length a wavelength or more, which, in turn, changes the comb element frequencies by $f_{\rm rep}$ or more. Although the long term drift of f_0 and $f_{\rm rep}$ caused by temperature changes can easily be compensated by the feedback loop, due to the actuator dynamic range, the duration of locking is limited. To obtain long-term locking, the laser is constructed on a 5-cm-thick cast aluminum plate. Typically, the thermal mass of such a plate is sufficient so that active temperature control is not required, although that depends to some extent on the ambient temperature fluctuations. A cavity mirror mounted on a piezo-electric transducer (PZT) with one wavelength worth of travel, together with thermal stabilization

via a gentle water flow through the laser base plate, can usually maintain feedback lock without interruption for many hours. A secondary benefit of the plate is a greater immunity to higher frequency (airborne) vibrations. By carefully isolating the cast plate (typically with rubber stoppers/springs having a resonant frequency of ~400 Hz) from the table and arranging the rigid enclosure to entirely span the cast plate, the airborne vibrations are not strongly coupled to the laser. Instead, for the most part, they are directly shorted to the optical table.

B. Generation of an Octave

As described in Section I-B, the simplest scheme for detection of f_0 requires an optical spectrum that spans an octave. Although KLM Ti:sapphire lasers generate remarkably broad spectra, they typically do not yield the necessary bandwidth. Note that our definition of spanning an octave is that useful ν-to-2ν beats can be produced, which can typically be achieved even when the ν and 2ν points are as far as 40 dB below the spectral peak. This is a substantially easier criterion than typically used, which might be based on 3 or even 10 dB points.

The prevalent means of obtaining an octave spanning spectrum is via nonlinear spectral broadening in microstructure fiber, which is used for all of the results presented herein. Microstructure fiber utilizes air holes, rather than a traditional doping of the core, to achieve the index difference needed for waveguiding. The resulting large index difference can produce a zero in the group velocity dispersion within the bandwidth of Ti:sapphire lasers. This *enables* in enormous spectral broadening [29], [30], to the point where the output is called a supercontinuum. There is substantial interest in understanding the supercontinuum generation process [31], [32]. Remarkably, the comb spectrum is largely preserved during this enormously nonlinear process, although excess noise is generated if insufficiently short input pulses are used. The excess noise arises from a combination of Raman processes and modulation instability seeded by vacuum fluctuation [33], [34]. Typically a signal-to-noise ratio of 30–40 dB is required for stable locking, so sufficient noise can prevent the lock; although, often it just degrades and increases the linewidth of f_0. Typically, satisfactory results are obtained for input pulses with durations of 30 fs or less.

The practical difficulties accompanying microstructure fiber have motivated attempts to obtain an octave spanning spectrum directly from mode-locked lasers. This was achieved by a combination of improved dispersion compensating mirrors and adding a second time and space focus in a nonlinear medium, which provided spectral broadening, to the laser cavity [18], [27]. Very large spectral bandwidth has also been obtained from high repetition rate ring cavities by a small change to the cavity to increase the strength of the self-focusing in the crystal [35]. Although measurable power was obtained at the octave points, it was insufficient to implement a ν-to- 2ν self-referencing scheme, requiring instead a 2ν-to- 3ν scheme [19].

C. Interferometer

An example of a ν-to- 2ν interferometer is shown in the lower left of Fig. 2. A dichroic beam splitter separates the ν and 2ν components, which for convenience in the example correspond to wavelengths of 1064 and 532 nm, respectively. The ν component is frequency doubled in a β-barium borate (BBO) crystal. The 2ν component is frequency shifted in an acousto-optic modulator (AOM). The frequency shift imparted by the AOM f_{AOM} moves the detected heterodyne beat (see below) and facilitates locking $\Delta\phi_{\mathrm{CE}} = 0$. The resulting beams, which now have similar wavelengths, are recombined in a polarizing beam splitter. The recombined beam is passed through an interference filter to select just the part of the spectrum where overlap occurs and is detected with a photodiode.

For optical frequency metrology and optical clock applications, f_{rep} must be locked. Generally, f_0 is locked as well, but there are schemes where it cancels, or it is simply counted. However, for simply maintaining carrier-envelope phase coherence, f_{rep} does not need to be locked if f_0 is coherently derived from it, or locked to 0. In the interferometer shown in Fig. 2, f_{AOM} must also be coherently derived from f_{rep}.

D. Control Parameters

Control of f_0 requires that there be laser parameters that affect it. Two widely used possibilities are swiveling the high reflector [3], [12], [36] and adjusting the pump power [1], [37]–[39]. Swiveling the high reflector relies on the fact that the spectrum is spatially dispersed across the mirror, thus this technique only works in lasers that use prisms for dispersion compensation; whereas, adjusting the pump power works in either a prism based laser or a prismless one that uses dispersion compensating mirrors.

Swiveling the high reflector following the intracavity prism sequence produces a small group delay, thereby changing the effective difference between group and phase velocities in the laser cavity, which, in turn, produces a change in ϕ_{CE} $(\Delta\phi_{\mathrm{CE}})$. The swivel of the high reflector results in a linear phase shift with frequency which is, by Fourier analysis, equivalent to a group delay. A more detailed analysis can be found in [12].

Empirically, changing the pump power has been shown to change f_0. However, the exact mechanism remains in question. Initial expectations were that the nonlinear phase shift in the crystal would cause $\Delta\phi_{\mathrm{CE}}$ to change; however, it was found that the sign of the change was incorrect [1]. This was attributed to a change in spectral position as a function of intensity. Further theoretical work showed that the nonlinear change in the group velocity also needs to be considered [40]. However, numerical simulations show that the results depend on the material properties [41]. More detailed experimental studies have clearly shown that spectral shifts occur and are well correlated with the resulting observed dynamics [38], [39].

III. Characterization of Phase Coherence

Optical frequency metrology and optical clock applications generally are sensitive to the frequency of individual comb lines. From (1), it is clear that fluctuations in f_{rep} dominate over those in f_0 because n is typically a large number on the order of 10^5 to 10^6. However, for time-domain applications, maintaining carrier-envelope phase coherence over long time scales is more important, which is determined by f_0. For example, if f_0 deviates

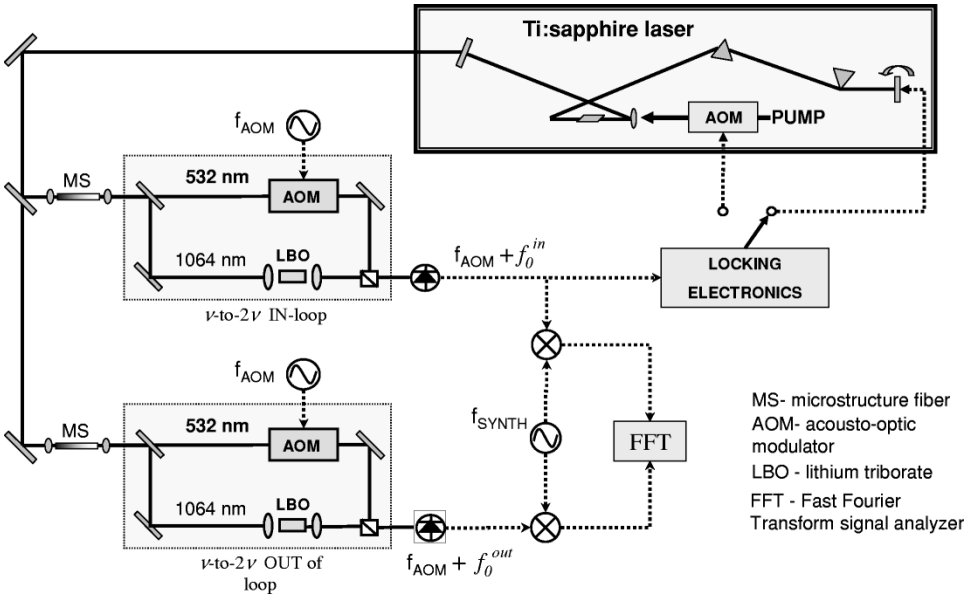

Fig. 3. Experimental setup showing how the coherence of $\phi_{\rm CE}$ is measured. Second ν-to- 2ν interferometer provides means for an out-of-loop measurement.

from the desired value by 1 Hz for a period of 1 s, the carrier-envelope phase will slip by a full 2π. More specifically, over a time interval $\tau_{\rm obs}$, the root mean square (rms) carrier-envelope phase fluctuations are

$$\Delta\phi_{\rm CE}^{\rm RMS}\big|_{\tau_{\rm obs}} = 2\sqrt{\int_{-\infty}^{(-1/\tau_{\rm obs})} \frac{S_{f_o}(f)}{f^2} df} = 2\sqrt{\int_{-\infty}^{(-1/\tau_{\rm obs})} S_{\phi_{\rm CE}}(f) df} \qquad (2)$$

where $S_{f_o}(f)$ is the power spectral density of the frequency fluctuations in f_0 and $S_{\phi_{\rm CE}}(f)$ is the phase noise spectrum of $\phi_{\rm CE}$ as a function of frequency f. The coherence time $\tau_{\rm coh}$ is typically defined as $\tau_{\rm obs}/2\pi$ for which $\Delta\phi_{\rm CE}^{\rm RMS}\sim 1$ rad.

A. Measurement

To measure the carrier-envelope phase coherence, side-by-side ν-to- 2ν interferometers are used, as shown in Fig. 3. One of the interferometers is used to lock f_0, while the other provides an independent measurement of it. Measurement of f_0 from the interferometer that is used to lock the laser is referred to as in-loop, whereas measurements using the second interferometer are called out-of-loop. The laser can be controlled by either tilting the high reflector or by adjusting the pump power via an AOM. In this section, the latter technique is used as it offers higher bandwidth than our original PZT used to swivel the high reflector.

Referring to Fig. 3, the phase noise spectrum of f_0 is determined, both in-loop and out-of-loop, by mixing the beat signal from the interferometers $(f_0 + f_{\rm aom})$ with the output of a frequency synthesizer $(f_{\rm synth})$. The offset frequency is locked to $f_0 = 0$ as in Section II. The mixing product is then analyzed on a fast Fourier transform (FFT) dynamic signal analyzer with a maximum bandwidth of 102.4 kHz and a minimum resolution of 244 μHz. We verified that the strength of the phase sidebands making up the spectrum is much less than 1 rad; this allows us to use a mixer as opposed to a frequency-to-voltage converter as a phase detector. First, we use the mixer by setting $f_{\rm synth} = f_{\rm aom}$, which mixes the heterodyne beats carrier to dc. This gives the baseband single-sideband noise spectrum of $S_{\phi_{\rm CE}}(f)$. To gain a more intuitive representation of the phase noise, we offset $f_{\rm synth}$ from $f_{\rm aom}$ by 50 kHz, which yields the full sideband noise spectrum. Although both measurements yield the same information, the latter is more intuitive as it shows the linewidth of f_0.

B. Results

Fig. 4 displays the results of both measurements [42]. In addition to $S_{\phi_{\rm CE}}(f)$, Fig. 4(a) also shows the accumulated carrier-envelope phase noise jitter, $\Delta\phi_{\rm CE}^{\rm RMS}$, as a function of $\tau_{\rm obs}$ (upper axis, increasing to left). Five spectra, of decreasing span and increasing resolution, were combined to obtain greater resolution close to dc. Integration from 102.4 kHz to 0.9765 mHz reveals $\Delta\phi_{\rm CE}^{\rm RMS}\sim 0.12$ rad in-loop and 0.72 rad out-of-loop. An unlocked spectrum, obtained using a frequency-to-voltage converter, is included to demonstrate the effectiveness of the feedback loop.

The linewidth of f_0 is shown in Fig. 4(b). For phase noise sidebands $\ll 1$ rad, the strength of the sidebands relative to the carrier directly approximates the phase modulation index (amplitude of the phase modulation). From these noise sidebands, $S_{\phi_{\rm CE}}(f)$ can be derived and integrated, confirming the baseband measurements presented above. The linewidth is still unresolved below 1.95 mHz for the in-loop and 0.976 mHz for the out-of-loop measurements. This shows that the feedback loop suppresses phase noise at very low frequency, yielding long-term phase coherence. Phase noise at higher frequencies (above 100 kHz) was not significant.

Although these results show that long term phase coherence is achievable, it would be desirable to improve it further. In Section IV, we look at the conversion of amplitude fluctuations to phase noise in the microstructure fiber used to generate an octave.

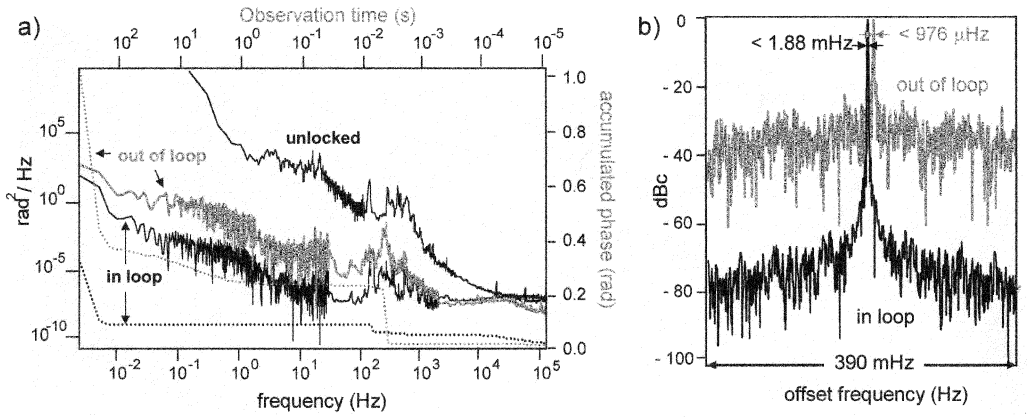

Fig. 4. (a) (left axis) In-loop and out-of-loop $S_{\phi_{\rm CE}}(f)$ versus offset frequency. (right axis) Accumulated phase jitter as function of observation time obtained by integration of $S_{\phi_{\rm CE}}(f)$. Stabilization process adds noise past ~5 KHz and roll-off in the out-of-loop spectrum at ~30 KHz is consistent with the stabilization servo bandwidth. An unlocked spectrum is included for comparison. (b) Spectrum of f_0 for both in-loop and out-of-loop linewidths. Curves are offset horizontally for clarity; both are resolution limited.

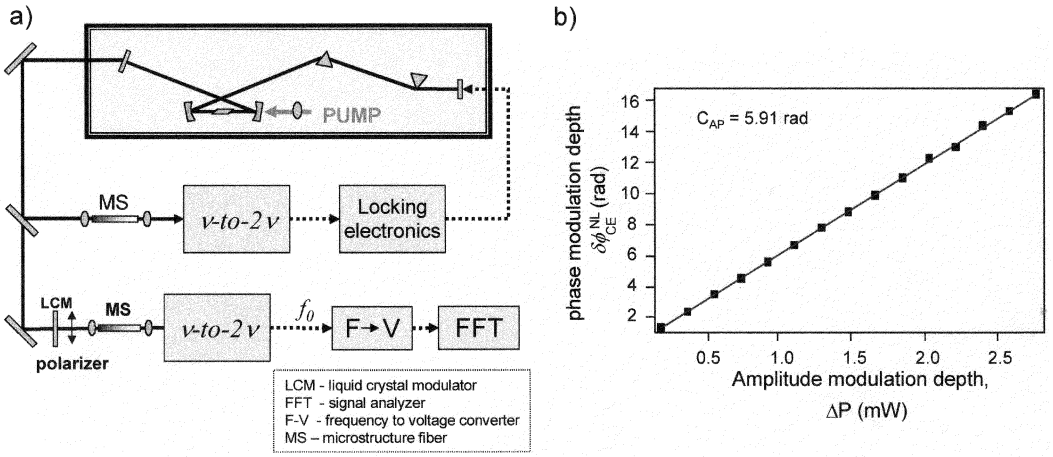

Fig. 5. (a) Experimental setup for measuring the conversion of amplitude fluctuations to phase noise in the microstructure fiber. Amplitude modulation is imposed on the laser power before MS fiber. Modulation frequency is 10 kHz, well outside the feedback bandwidth (1 kHz). Laser is stabilized using a second v-to-$2v$ interferometer. (b) Results of the measurement showing the amplitude of the phase fluctuations as function of the amplitude modulation depth.

IV. Amplitude to Phase Noise Conversion in Microstructure Fiber

The very high effective Kerr nonlinearity of the microstructured fiber is essential for obtaining strong nonlinear broadening required to obtain an octave spanning spectrum. However, concomitant with this positive feature is the unfortunate effect that it will also convert amplitude fluctuations into phase fluctuations. The Kerr nonlinearity means that the index of refraction n depends on the light intensity, i.e., $n(I) = n_0 + n_2 I$, where n_0 is the linear index, n_2 is the Kerr coefficient, and I is the effective intensity of the light in the core, including the effective area. The net carrier-envelope phase shift for light with frequency ω and intensity I after propagation through a distance l_0 is

$$\begin{aligned}\delta\phi_{\rm CE} &= \frac{\omega l_0}{c}\left(n_g - n\right)\\ &= \frac{\omega l_0}{c}\left(\omega\frac{dn_0}{d\omega} + I\left(t\right)\omega\frac{dn_2}{d\omega}\right)\\ &= \delta\phi^0_{\rm CE} + \delta\phi^{NL}_{\rm CE}\left(t\right)\end{aligned} \tag{3}$$

where the group velocity $n_g = n + \omega dn/d\omega$ and c is the speed of light. The linear dispersion results in a constant shift in the carrier-envelope phase given by $\delta\phi^0_{\rm CE}$, which does not affect f_0 as it is the same for all of the pulses, and f_0 depends on pulse-to-pulse changes in the $\phi_{\rm CE}$. However, if the intensity is time varying, then so too will be the nonlinear contribution $\delta\phi^{NL}_{\rm CE}$, which will change the pulse-to-pulse phase and hence f_0. From (3), we rewrite the nonlinear phase shift as

$$\delta\phi^{NL}_{\rm CE} = \frac{\omega^2 l_0}{c}\frac{dn_2}{d\omega}\Delta I = C_{\rm AP}\Delta P \tag{4}$$

where this equation defines $C_{\rm AP}$, the amplitude-to-phase conversion coefficient and ΔP is a change in the optical power.

To measure $C_{\rm AP}$, we impose a sinusoidal amplitude modulation on the laser power using a liquid crystal modulator prior to coupling into the microstructure fiber, as shown in Fig. 5(a). This amplitude modulation is converted to a carrier-envelope phase modulation according to (4). The carrier-envelope phase of the output of microstructure fiber is detected with a standard ν-to- 2ν interferometer, yielding a modulated f_0, $f_o^{NL} = (1/2\pi)\omega_{\rm m} C_{\rm AP}\Delta P\cos(\omega_{\rm m} t)$ where $\omega_{\rm m}$ is the frequency of the amplitude modulation imposed on the input to the fiber. A frequency-to-voltage converter is used to determine the resulting frequency modulation depth, enabling us to then calculate the

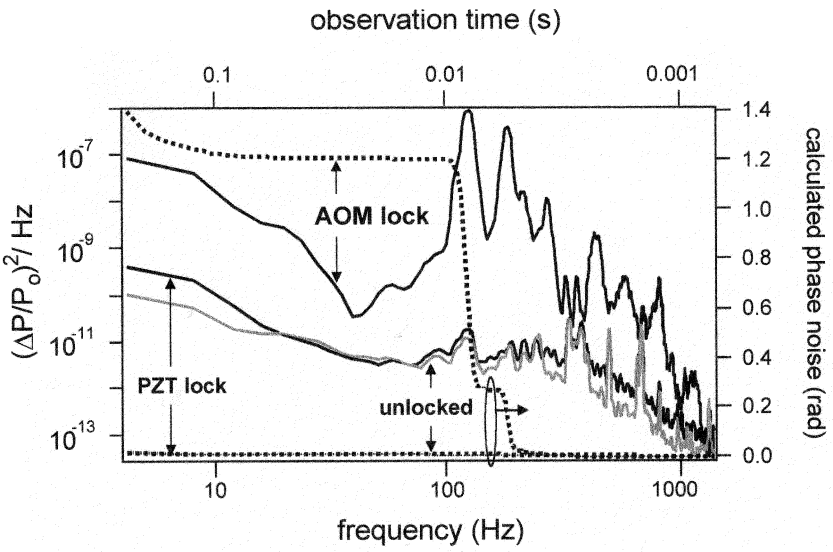

Fig. 6. (left axis) Spectrum of the amplitude fluctuations when the laser is unlocked, locked using an AOM in the pump beam and locked using the fast PZT. (right axis) Accumulated phase jitter determined by using the measured $C_{\rm AP}$ and integrating the phase fluctuation spectrum obtained from the amplitude fluctuation spectrum.

carrier-envelope phase modulation. The resulting phase modulation depth as a function of amplitude modulation depth is plotted in Fig. 5(b). The linear fit yields a $C_{\rm AP} = 5.91$ rad/mw or 591 rad/nJ. These measurements were taken at $\omega_{\rm m} = 10$ kHz on a 4.5-cm-long fiber with an average coupled power of 50 mW from a 100-MHz repetition rate laser. The spectral width of the laser was approximately 50 nm, although the value of $C_{\rm AP}$ does not depend strongly on the laser bandwidth. Dispersion compensation was employed to deliver a pulse with minimum to slightly normal chirp at the fiber input. Measurements at various values of $\omega_{\rm m}$ yielded similar results for $C_{\rm AP}$, as do measurements at very low modulation frequencies using side-by-side interferometers [43].

The conversion of amplitude fluctuations to phase fluctuations in the microstructure fiber will add phase noise to the carrier-envelope phase of pulses generated by the stabilized laser. This occurs because the feedback loop will mistakenly attempt to correct for the apparent phase fluctuations which are, in fact, an artifact as they are generated outside the laser cavity. Thus, it is important to know the conversion strength, which, together with a measure of the amplitude fluctuations in the output of the laser, yields an estimate of the resulting phase fluctuations. This estimation is carried out in Section V.

V. Improvement of Phase Coherence

Given our understanding of the effect of amplitude noise, we can now investigate the source of the remaining phase noise in results presented in Section III. Fig. 6 shows the power spectrum of the amplitude fluctuations of the laser when locked using an AOM as in Section III and when the laser is unlocked. The amplitude noise actually increases when the laser is locked. This is contrary to results on a prismless laser, which showed that the amplitude noise decreases when $\Delta\phi_{\rm CE}$ was locked [37]. Presumably, these contrary findings are due to differing sources of noise in the two cases. In the case of lasers that use prisms, it has been suggested that beam pointing instability is a source of significant phase noise [44], although we have not observed this effect in our lasers. If we convert the amplitude fluctuations to phase fluctuations using the value of $C_{\rm AP}$ obtained in Section IV, and integrate it to obtain an estimated $\Delta\phi_{\rm CE}^{\rm RMS}$, we obtain the dotted line shown in Fig. 6, which shows an alarmingly large phase jitter. Indeed, this estimate is larger than the out-of-loop results shown above, which suggests that there is some cancellation of amplitude to phase noise conversion in the two pieces of microstructure fiber via common mode noise.

To avoid the amplitude fluctuations due to the AOM, we revisit the idea of swiveling the high reflector. The motivation for using an AOM was to obtain a large servo bandwidth. However, with a carefully designed PZT system that uses a small mirror mounted on two small disc PZTs driven in opposition, we are able to obtain a servo bandwidth of close to 25 kHz, which is comparable to that required when stabilizing with the AOM. The resulting amplitude noise when locked using the PZT is almost identical to that for an unlocked laser (Fig. 6), and the estimated $\Delta\phi_{\rm CE}^{\rm RMS}$ due to amplitude to phase conversion is entirely negligible.

Using the improved PZT, we now repeat the measurements of phase coherence. Fig. 7 shows the in-loop, out-of-loop, and unlocked results. These results yield a phase coherence time of greater than 326 s, which is measurement limited.

VI. Extra Cavity Control of $\phi_{\rm CE}$

Having achieved such long phase coherence, it is interesting to start exploring issues related to controlling the carrier-envelope phase, $\phi_{\rm CE}$, itself rather than just its evolution. A careful derivation of f_0 shows that the phase of the heterodyne beat is directly related to $\phi_{\rm CE}$[16]. However, by using an interferometer that sends the ν and 2ν components through distinct paths, there is an arbitrary phase shift between the two that adds an unknown offset to the phase of f_0. Even with an interferometer that does not use distinct paths, material dispersion, including that of air, easily causes significant phase shifts, as we show below.

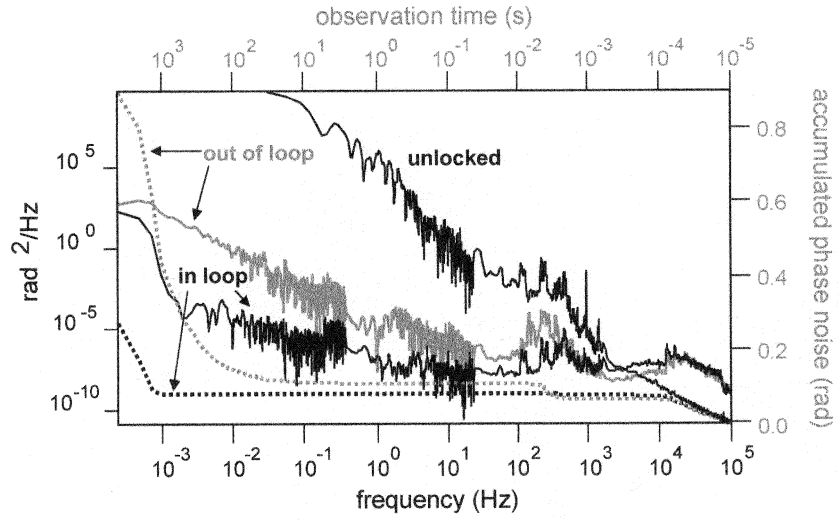

Fig. 7. (left axis) Phase noise spectrum as measured in- and out-of-loop using the fast PZT. (right axis) Accumulated phase jitter obtained by integrating the spectra for the two locked cases. Unlocked phase noise spectrum is included to indicate noise supression.

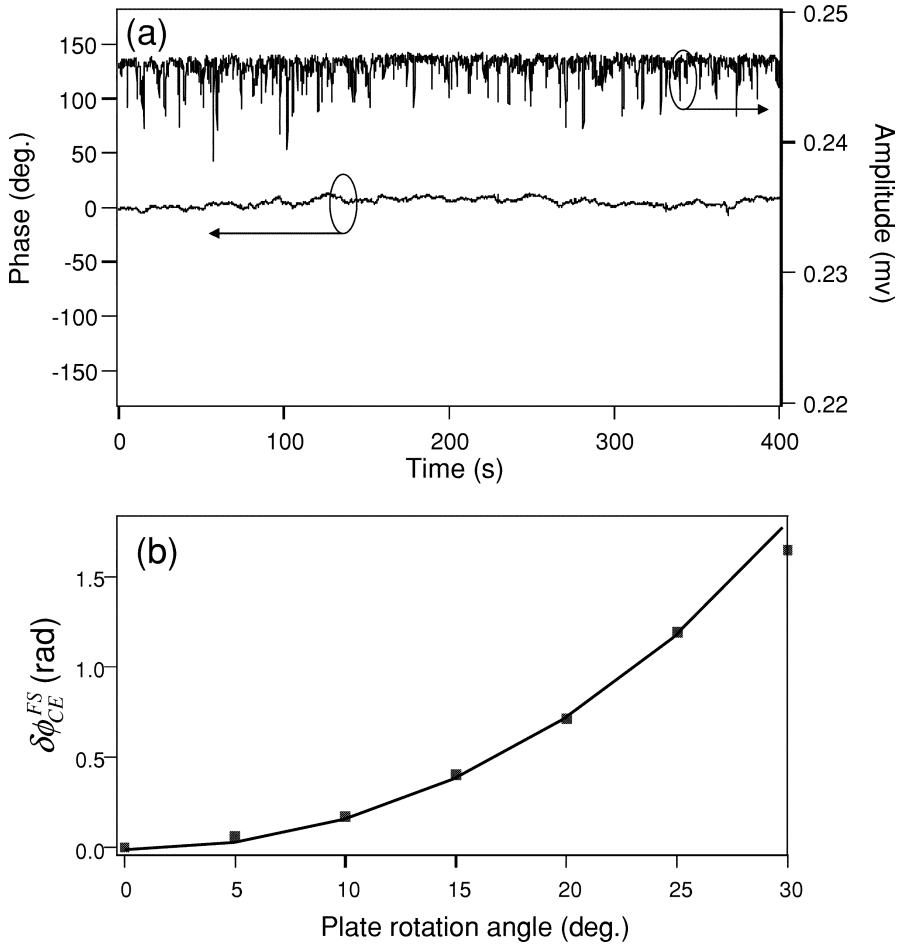

Fig. 8. (a) Amplitude and phase of the f_0 signal from the second interferometer measured employing a lock-in referenced to the signal used to lock the laser with the first interferometer. Phase of this signal is ϕ_{CE} modulo an offset. (b) Phase offset induced by a 178-μm thick fused silica plate as a function of the rotation angle of the plate, 0° is perpendicular to the beam. Squares are the experimental points and the solid line shows calculations based on the dispersion of fused silica.

To measure the phase of the beat signal, we use a dual interferometer setup similar to that shown in Fig. 3. As before, the first interferometer is used to lock the laser, but in this case, f_0 is locked to an offset frequency of 50 kHz. The output of the second interferometer is monitored using a dual phase lock-in amplifier, which is referenced to the 50-kHz signal used to lock the f_0. The lock-in then provides a measure of the phase of f_0 (relative to the 50-kHz reference signal). A data run taken over

400 s is shown in Fig. 8(a). The standard deviation of the phase over this time is 3.8 degrees (0.07 rad) with a maximum deviation of 20.8 deg (0.35 rad). These results directly demonstrate the very good carrier-envelope phase coherence of the pulse train.

To confirm that the phase of f_0 represents a measure of ϕ_{CE}, we inserted a 178-μm-thick fused silica plate in the beam before it entered the second interferometer. The plate is then rotated and due to changes in the path length of the plate, the material dispersion of the silica will cause ϕ_{CE} to change. We monitor the phase of f_0 during rotation. The results are shown in Fig. 8(b). The solid line is a calculation based on the known dispersion of fused silica. Note that a measurable phase shift occurs for a rotation angle of only 5°, which corresponds to a change in the material thickness of only 0.3 μm. This shows that the phase is exquisitely sensitive to dispersion, but at the same time it shows that it can easily be controlled external to the cavity, for example by mounting the plate on a galvometer.

VII. Conclusion

The progress in building phase stabilized mode-locked lasers has allows phase coherence to be preserved over a very long time. Achieving this has been aided by understanding the contribution of amplitude to phase conversion in the microstructure fiber. An improved PZT actuator eliminated the additional phase noise that we observed when modulating the pump power to obtain phase stabilization. Based on these results, we have directly shown the phase stability and its sensitivity to propagation through dispersive materials.

Acknowledgment

The authors would like to acknowledge the contributions of J. Hall to this work and R.W. Windeler (OFS Labs) for providing the microstructure fiber.

References

[1] L. Xu, C. Spielmann, A. Poppe, T. Brabec, F. Krausz, and T. W. Hänsch, "Route to phase control of ultrashort light pulses," *Opt. Lett.*, vol. 21, pp. 2008–2010, 1996.

[2] H. R. Telle, G. Steinmeyer, A. E. Dunlop, J. Stenger, D. H. Sutter, and U. Keller, "Carrier-envelope offset phase control: A novel concept for absolute optical frequency control and ultrashort pulse generation," *Appl. Phys. B*, vol. 69, pp. 327–332, 1999.

[3] D. J. Jones, S. A. Diddams, J. K. Ranka, A. Stentz, R. S. Windeler, J. L. Hall, and S. T. Cundiff, "Carrier-envelope phase control of femtosecond mode-locked lasers and direct optical frequency synthesis," *Science*, vol. 288, pp. 635–639, 2000.

[4] A. Apolonski, A. Poppe, G. Tempea, C. Spielmann, T. Udem, R. Holzwarth, T. W. Hänsch, and F. Krausz, "Controlling the phase evolution of few-cycle light pulses," *Phys. Rev. Lett.*, vol. 85, pp. 740–743, 2000.

[5] R. J. Jones and J. C. Diels, "Stabilization of femtosecond lasers for optical frequency metrology and direct optical to radio frequency synthesis," *Phys. Rev. Lett.*, vol. 86, pp. 3288–3291, 2001.

[6] S. A. Diddams, D. J. Jones, J. Ye, T. Cundiff, J. L. Hall, J. K. Ranka, R. S. Windeler, R. Holzwarth, T. Udem, and T. W. Hänsch, "Direct link between microwave and optical frequencies with a 300 thz femtosecond laser comb," *Phys. Rev. Lett.*, vol. 84, pp. 5102–5105, 2000.

[7] R. Holzwarth, T. Udem, T. W. Hänsch, J. C. Knight, W. J. Wadsworth, and P. S. J. Russell, "Optical frequency synthesizer for precision spectroscopy," *Phys. Rev. Lett.*, vol. 85, pp. 2264–2267, 2000.

[8] J. Ye, J. L. Hall, and S. A. Diddams, "Precision phase control of ultrawide bandwidth fs laser—A network of ultrastable frequency marks across the visible spectrum," *Opt. Lett.*, vol. 25, p. 1675, 2000.

[9] J. Stenger, T. Binnewies, G. Wilpers, F. Riehle, H. R. Telle, J. K. Ranka, R. S. Windeler, and A. J. Stentz, "Phase-coherent frequency measurement of the ca intercombination line at 657 nm with a Kerr-lens mode-locked femtosecond laser," *Phys. Rev. A*, vol. 6302, p. 021 802, 2001.

[10] J. Stenger, C. Tamm, N. Haverkamp, S. Weyers, and H. R. Telle, "Absolute frequency measurement of the $171\mathrm{yb}+$ clock transition with a Kerr-lens mode-locked femtosecond laser," *Opt. Lett.*, vol. 26, pp. 1589–1591, 2001.

[11] T. Udem, S. A. Diddams, K. R. Vogel, C. W. Oates, E. A. Curtis, W. D. Lee, W. M. Itano, R. E. Drullinger, J. C. Bergquist, and L. Hollberg, "Absolute frequency measurements of the hg^+ and ca optical clock transitions with a femtosecond laser," *Phys. Rev. Lett.*, vol. 86, pp. 4996–4999, 2001.

[12] S. T. Cundiff, J. Ye, and J. L. Hall, "Optical frequency synthesis based on mode-locked lasers," *Rev. Sci. Instrum.*, vol. 72, pp. 3749–3771, 2001.

[13] S. A. Diddams, T. Udem, J. C. Bergquist, E. A. Curtis, R. E. Drullinger, L. Hollberg, W. M. Itano, W. D. Lee, C. W. Oates, K. R. Vogel, and D. J. Wineland, "An optical clock based on a single trapped hg-$199(+)$ ion," *Science*, vol. 293, pp. 825–828, 2001.

[14] J. Ye, L.-S. Ma, and J. L. Hall, "Molecular iodine clock," *Phys. Rev. Lett.*, vol. 87, p. 270 801, 2001.

[15] G. Wilpers, T. Binnewies, C. Degenhardt, U. Sterr, J. Helmcke, and F. Riehle, "Optical clock with ultracold neutral atoms," *Phys. Rev. Lett.*, vol. 89, p. 230 801, 2002.

[16] S. T. Cundiff, "Phase stabilization of ultrashort optical pulses," *J. Phys. D.*, vol. 35, pp. R43–R59, 2002.

[17] T. Brabec and F. Krausz, "Intense few-cycle laser fields: Frontiers of nonlinear optics," *Rev. Mod. Phys.*, vol. 72, pp. 545–591, 2000.

[18] U. Morgner, R. Ell, G. Metzler, T. R. Schibli, F. X. Kartner, J. G. Fujimoto, H. A. Haus, and E. P. Ippen, "Nonlinear optics with phase-controlled pulses in the sub-two-cycle regime," *Phys. Rev. Lett.*, vol. 86, pp. 5462–5465, 2001.

[19] T. M. Ramond, S. A. Diddams, L. Hollberg, and A. Bartels, "Phase-coherent link from optical to microwave frequencies by means of the broadband continuum from a 1-GHz Ti: Sapphire femtosecond oscillator," *Opt. Lett.*, vol. 27, pp. 1842–1844, 2002.

[20] D. E. Spence, P. N. Kean, and W. Sibbett, "60-fsec pulse generation from a self-mode-locked ti-sapphire laser," *Opt. Lett.*, vol. 16, pp. 42–44, 1991.

[21] D. K. Negus, L. Spinelli, N. Goldblatt, and G. Feugnet, "Sub-100 femtosecond pulse generation by Kerr lens mode-locking in Ti: $\mathrm{Al_2O_3}$," Advanced Solid-State Lasers, 1991, to be published.

[22] R. L. Fork, O. E. Martinez, and J. P. Gordon, "Negative dispersion using pairs of prisms," *Opt. Lett.*, vol. 9, pp. 150–152, 1984.

[23] M. T. Asaki, C. P. Huang, D. Garvey, J. P. Zhou, H. C. Kapteyn, and M. M. Murnane, "Generation of 11-fs pulses from a self-mode-locked ti-sapphire laser," *Opt. Lett.*, vol. 18, pp. 977–979, 1993.

[24] R. Szipocs, K. Ferencz, C. Spielmann, and F. Krausz, "Chirped multilayer coatings for broad-band dispersion control in femtosecond lasers," *Opt. Lett.*, vol. 19, pp. 201–203, 1994.

[25] F. X. Kärtner, U. Morgner, T. Schibli, J. G. Fujimoto, E. P. Ippen, V. Scheuer, G. Angelow, and T. Tschudi, *Ultrabroadband double-chirped mirror pairs for single-cycle pulse generation*, 2000.

[26] U. Morgner, F. X. Kärtner, S. H. Cho, Y. Chen, H. A. Haus, J. G. Fujimoto, E. P. Ippen, V. Scheuer, G. Angelow, and T. Tschudi, "Sub-two-cycle pulses from a Kerr-lens mode-locked Ti: Sapphire laser," *Opt. Lett.*, vol. 24, pp. 411–413, 1999.

[27] R. Ell, U. Morgner, F. X. Kärtner, J. G. Fujimoto, E. P. Ippen, V. Scheuer, G. Angelow, T. Tschudi, M. J. Lederer, A. Boiko, and B. Luther-Davies, "Generation of 5 fs pulses and octave-spanning spectra directly from a ti:Sapphire laser," *Opt. Lett.*, vol. 26, pp. 373–375, 2001.

[28] A. Bartels, T. Dekorsy, and H. Kurz, "Femtosecond ti:Sapphire ring laser with a 2-GHz repetition rate and its application in time-resolved spectroscopy," *Opt. Lett.*, vol. 24, pp. 996–998, 1999.

[29] J. K. Ranka, R. S. Windeler, and A. J. Stentz, "Visible continuum generation in air-silica microstructure optical fibers with anomalous dispersion at 800 nm," *Opt. Lett.*, vol. 25, pp. 25–27, 2000.

[30] ——, "Optical properties of high-delta air-silica microstructure optical fibers," *Opt. Lett.*, vol. 25, pp. 796–798, 2000.

[31] J. Herrmann, U. Griebner, N. Zhavoronkov, A. Husakou, D. Nickel, J. C. Knight, W. J. Wadsworth, P. S. J. Russell, and G. Korn, "Experimental evidence for supercontinuum generation by fission of higher-order solitons in photonic fibers," *Phys. Rev. Lett.*, vol. 88, p. 173 901, 2002.

[32] A. L. Gaeta, "Nonlinear propagation and continuum generation in microstructured optical fibers," *Opt. Lett.*, vol. 27, pp. 924–926, 2002.
[33] K. L. Corwin, N. R. Newbury, J. M. Dudley, S. Coen, S. A. Diddams, K. Weber, and R. S. Windeler, "Fundamental noise limitations to supercontinuum generation in microstructure fiber," *Phys. Rev. Lett.*, vol. 90, p. 113 904, 2003.
[34] J. N. Ames, S. Ghosh, R. S. Windeler, A. L. Gaeta, and S. T. Cundiff, "Excess noise generation during spectral broadening in microstructure fiber," *Appl. Phys. B*, vol. 77, pp. 279–284, 2003.
[35] A. Bartels and H. Kurz, "Generation of a broadband continuum by a Ti: Sapphire femtosecond oscillator with a 1-GHz repetition rate," *Opt. Lett.*, vol. 27, pp. 1839–1841, 2002.
[36] T. Udem, J. Reichert, R. Holzwarth, and T. W. Hänsch, "Absolute optical frequency measurement of the cesium d-1 line with a mode-locked laser," *Phys. Rev. Lett.*, vol. 82, pp. 3568–3571, 1999.
[37] A. Poppe, R. Holzwarth, A. Apolonski, G. Tempea, C. Spielmann, T. W. Hansch, and F. Krausz, "Few-cycle optical waveform synthesis," *Appl. Phys. B*, vol. 72, p. 977, 2001.
[38] K. W. Holman, R. J. Jones, A. Marian, S. T. Cundiff, and J. Ye, "Intensity-related dynamics of femtosecond frequency combs," *Opt. Lett.*, vol. 28, pp. 851–853, 2003.
[39] ——, "Detailed studies and control of intensity-related dynamics of femtosecond frequency combs from mode-locked ti:Sapphire lasers," *IEEE J. Select. Topics Quantun Electron.*, submitted for publication.
[40] H. A. Haus and E. P. Ippen, "Group velocity of solitons," *Opt. Lett.*, vol. 26, pp. 1654–1656, 2001.
[41] P. Goorjian, private communication, 2003.
[42] T. M. Fortier, D. J. Jones, J. Ye, S. T. Cundiff, and R. S. Windeler, "Long-term carrier-envelope phase coherence," *Opt. Lett.*, vol. 27, pp. 1436–1438, 2002.
[43] T. M. Fortier, J. Ye, S. T. Cundiff, and R. S. Windeler, "Nonlinear phase noise generated in air-silica microstructure fiber and its effect on carrier-envelope phase," *Opt. Lett.*, vol. 27, pp. 445–447, 2002.
[44] F. W. Helbing, G. Steinmeyer, U. Keller, R. S. Windeler, J. Stenger, and H. R. Telle, "Carrier-envelope offset dynamics of mode-locked lasers," *Opt. Lett.*, vol. 27, pp. 194–196, 2002.

Tara M. Fortier received the B.Sc. degree in pure physics from Concordia University, Montreal, QC, Canada, in 1998. Her undergraduate thesis work was performed at the NRC in Ottawa, Canada, under the supervision of Dr. M. lvanov. She is currently working toward the Ph.D. degree in physics at JILA, University of Colorado, Boulder, under the tutelage of Dr. S. T. Cundiff.

David J. Jones was born in Colorado in 1969. He received the B.S. degree in physics and the B.S. degree in engineering from Swarthmore College in 1993. In 1994, he received the M. Phil. degree in engineering from the University of Cambridge, U.K. In 1998, he received the Ph.D. degree in electrical engineering from the Massachusetts Institute of Technology, Cambridge, MA.

Under a NIST-National Research Council associateship award, he completed his post-doctoral work at JILA in the University of Colorado, Boulder, from 1998 to 2000. After spending one year at PhotonEx, he returned to JILA as a Senior Research Associate. His current research interests include stabilization of ultrafast lasers for phase-sensitive ultrafast optics, optical frequency metrology, and other emerging applications.

Jun Ye born on Nov. 7, 1967, in Shanghai, China. He received the Ph.D. degree from the University of Colorado, Boulder, in 1997.

He is a fellow of JILA (a joint institute of the National Institute of Standards and Technology and the University of Colorado), Boulder. He leads a team of researchers who are working in areas including high-precision measurement, high-resolution and ultrasensitive laser spectroscopy, optical frequency metrology, ultrafast optics, cooling and trapping of atoms and molecules, and quantum dynamics in optical and atomic physics. He has co-authored over 100 technical papers and is a recipient of a number of awards from professional societies and agencies.

S. T. Cundiff received the B.A. degree in physics from Rutgers University, New Brunswick, NJ, in 1985. In 1992, he received the Ph.D. degree in applied physics from the University of Michigan, Ann Arbor.

He worked for two years at SciTec, Inc. in Princeton, N.J. In 1993 and 1994, he was a von Humboldt post-doctoral Fellow at Philipps University, Marburg, Germany. He was a post-doctoral Member of Technical Staff in the Advanced Photonics Research Department, Bell Labs, Lucent Technologies, Holmdel, NJ, from 1995 to 1997. Currently, he is a Physicist in the Quantum Physics Division, National Institute of Standards and Technology (NIST) and a Fellow of JILA, a joint institute between NIST and the University of Colorado, Boulder. He is also an Adjoint Faculty Member in the Department of Physics and Department of Electrical and Computer Engineering, University of Colorado.